Quantitative Neuroscience

Dr. Garrett Stanley

Modeling the Role of Excitatory and Inhibitory Conductances in L6CT Synchrony and its Effect on LFP Oscillations

---

Group 1

Minjae Chung, John Davis, Brady Souma

12/06/2025

Abstract:

The integration of control theory and neuroscience has demonstrated substantial potential to improve sensory processing outcomes. Recent experimental work by Dimwamwa et al. [1] suggests that the synchrony of Layer 6 corticothalamic (L6CT) neurons—rather than their firing rate alone—plays a central role in gating sensory signals to the ventral posteromedial nucleus (VPm). While biological studies have observed this "window of opportunity" phenomenon, they cannot easily isolate the specific excitatory and inhibitory conductances that drive it. In this study, we developed a conductance-based Leaky Integrate-and-Fire (LIF) computational model to strictly control and analyze these dynamics. We simulated a thalamocortical circuit driven by 35 synthetic L6CT neurons with tunable synchrony parameters. Our model successfully replicated the biological findings, demonstrating that increasing input synchrony (from 0.0 to 0.9 correlation) shifts the circuit from a suppressive state to an enhanced state, independent of the mean firing rate. Furthermore, we utilized this framework to analyze the precise timing of excitatory and inhibitory conductances and extended the model to simulate how these thalamic dynamics drive high-gamma Local Field Potential (LFP) oscillations in the cortex, based on findings from Russo et al. [2].

1. Introduction

In the field of neuroscience, understanding how the neocortex shapes thalamic processes remains one of the central challenges. Sensory thalamic regions, such as the ventral posteromedial nucleus (VPm), do not operate as simple relays but are instead governed by complex feedback loops involving cortical Layer 6 corticothalamic (L6CT) neurons and the inhibitory thalamic reticular nucleus (TRN). Historically, increases in L6CT firing were thought to directly correlate with stronger thalamic inhibition. However, recent research indicates that the timing and synchrony of L6CT spikes, not merely their average firing rate, determine whether VPm neurons are suppressed or excited.

Dimwamwa et al. [1] demonstrated this via a "window of opportunity" concept, where L6CT excitation and the delayed TRN inhibition create an optimal temporal window for spiking. While the biological data reveal this phenomenon clearly, experimental limitations make it difficult to directly measure the specific excitatory and inhibitory conductances or isolate the contributions of timing versus amplitude.

To address this, we developed a computational thalamocortical model consisting of VPm and TRN nodes driven by a population of synthetic L6CT spike trains. The objectives of this study were two-fold:

1. **Replication:** To reproduce the "window of opportunity" mechanism by generating L6CT inputs with precisely controlled synchrony independent of firing rate.
2. **Extension:** To analyze fundamental variables not directly measured in the biological paper, specifically the spike-triggered conductances, and to model the downstream effects of this synchrony on Local Field Potential (LFP) oscillations.

2. Background and Computational Framework Integration Methods

2.1 Thalamocortical Circuit Dynamics

The core circuit modeled in this study consists of three nodes: the excitatory L6CT input population, the inhibitory TRN, and the excitatory VPm. The anatomical connectivity dictates that L6CT neurons excite both the TRN and VPm. Crucially, the TRN provides feedforward inhibition to the VPm. This creates a "race condition" where the VPm must fire in response to L6CT excitation before the inhibitory conductance from the TRN arrives.

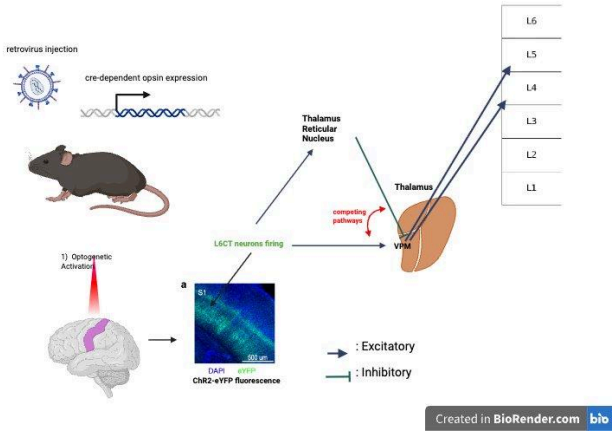

Figure 1: *Theoretical schematic of the thalamocortical circuit. L6CT neurons provide direct excitation to the VPm and disynaptic inhibition via the TRN.(**Created with BioRender.com**)*

2.2 Model Implementation (LIF)

To replicate the circuit dynamics observed in vivo, we utilized a conductance-based Leaky Integrate-and-Fire (LIF) framework. The state of the neurons in TRN and VPM compartments are separately governed by the following differential equation:

$$C_i \frac{dV_i}{dt} = G_{L,i}(E_{L,i} - V_i) + g_i^{CT}(E_{exc} - V_i) + g_i^{noise}(E_{exc} - V_i) + g_i^{TRN \to VPm}(E_{inh} - V_i)$$

Where g_i^{cT} represents the excitatory conductance driven by L6CT spikes and $g_i^{TRN \to Pm}$ represents the inhibitory conductance from the TRN . The biophysical parameters (capacitance, leak, and reversal potentials) were derived from the LIF backbone used in Dimwamwa et al. [1].

2.3 Algorithmic Generation of Synchrony

A critical innovation in our model is the strict decoupling of firing rate from synchrony. In biological experiments, increasing LED intensity often changes both. To isolate synchrony computationally, we implemented a custom algorithm to generate synthetic L6CT population activity.

We modeled the input as a population of N=35 neurons. For each time step dt, we generated spikes using a Bernoulli process derived from two sources:

1. **A Shared Source:** A single boolean array representing a "common" spike train, generated with probability $R \cdot dt$, where R is the target firing rate.
2. **Independent Sources:** A unique boolean array for each of the 35 neurons, also generated with probability $R \cdot dt$.

To construct the final spike train for neuron i, we combined these sources using bitwise logic controlled by the synchrony parameter SharedProbability (ranging from 0.0 to 1.0).

```python
def poisson_process(rate, duration, tStep):
    """
    Generates a boolean spike train from a homogeneous Poisson process.
    - rate (Hz): Firing rate
    - duration (s): Total time
    - tStep (s): Time step
    Returns: 1D boolean array (True at time of a spike)
    """
    num_steps = int(duration / tStep)
    # Probability of a spike in any given time bin
    prob = rate * tStep
    # Generate random numbers and compare to probability
    return np.random.rand(num_steps) < prob
```

```python
num_steps = int(duration / tStep)

# Store all trials in 3d array
all_trials_spike_trains: np.array = np.zeros((nTrials, num_neurons, num_steps), dtype=bool)

for trial in range(nTrials):
    # 1. Create one "shared" spike train
    shared_train = poisson_process(rate, duration, tStep)

    # 2. Create spike trains for each neuron
    all_spike_trains_this_trial = np.zeros((num_neurons, num_steps), dtype=bool)

    for i in range(num_neurons):
        # 3. Create a unique "independent" train
        ind_train = poisson_process(rate, duration, tStep)

        # 4. Randomly select spikes from shared train
        shared_spikes_used = (shared_train) & (np.random.rand(num_steps) < sharedProb)

        # 5. Randomly select spikes from independent train
        ind_spikes_used = (ind_train) & (np.random.rand(num_steps) < (1.0 - sharedProb))

        # 6. Combine them. A spike occurs if it's in *either* set.
        all_spike_trains_this_trial[i] = shared_spikes_used | ind_spikes_used

    all_trials_spike_trains[trial] = all_spike_trains_this_trial

return all_trials_spike_trains
```

Code Block 1: *Python implementation of the L6CT spike train generation. The algorithm uses a shared probability parameter to mix common and independent Poisson processes.*

This boolean logic ensures that as SharedProb increases, the proportion of spikes derived from the common source increases, creating vertical banding in the raster plot (synchrony), while the total spike count over the trial remains statistically constant .

3. Results

3.1 Validation of Synchrony Control

To validate our computational implementation, we first visualized the synthetic L6CT spike trains across different synchrony conditions. **Figure 2** displays the raster plots for the population of 35 synthetic L6CT neurons. The red dashed line indicates the stimulation onset (t=0.75 s), separating the silent baseline period from the active stimulation window.

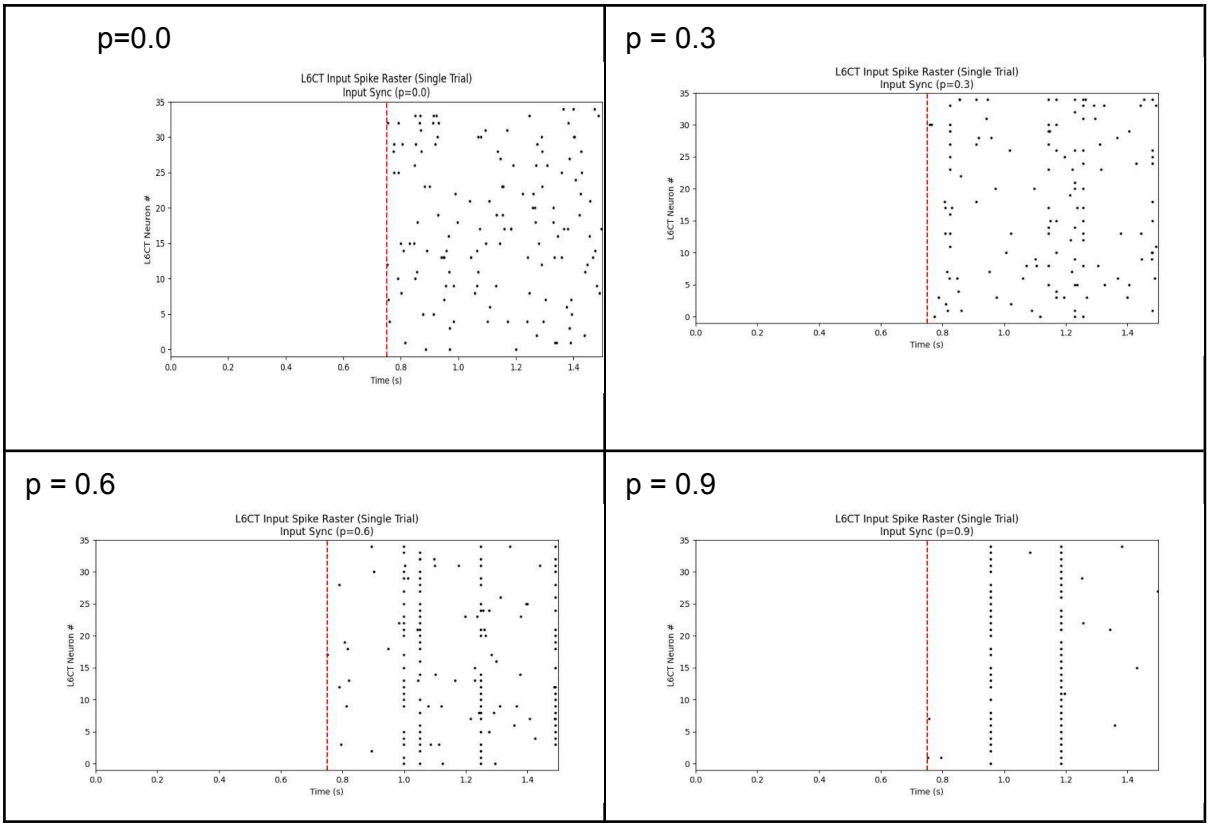

Figure 2: L6CT Input Spike Rasters across Synchrony Levels. The panels display spike times for 35 synthetic neurons. The red dashed line marks the separation of start time (t=0.75s). Note that the "Input Sync" (p) value indicated above each panel corresponds directly to the sharedProb parameter used in the model algorithm to control the probability of coincident spiking. At p=0.0, spikes are randomly distributed after onset. As SharedProb increases to 0.9, clear vertical banding emerges, indicating high temporal alignment (synchrony) despite the firing rate remaining constant.

The precise timing of the stimulation onset was enforced using a boolean temporal mask within the simulation loop. This ensured that L6CT contributions to the conductance equations were strictly gated to the "hold" phase of the experimental protocol.

```
start_step = int(config['ctStartTime'] / tStep)
time_mask = np.zeros(num_steps, dtype=bool)
time_mask[start_step:] = True # Only allow spikes AFTER start_step
```

Code Block 2: Python implementation of the temporal mask. The time_mask array ensures that L6CT spikes are only generated and integrated into the model after the defined ctStartTime

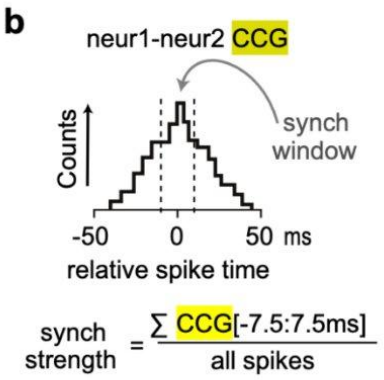

Quantitative Verification: To confirm that our Poisson-based algorithm successfully decoupled firing rate from synchrony, we validated the model outputs using the same metric applied in the biological study. Following the methodology of Dimwamwa et al. [1], we computed the **Synchrony Strength** for pairs of synthetic L6CT neurons. This metric is defined as the proportion of spikes falling within a ±7.5 ms window in the Cross-Correlogram (CCG) in the paper.

We swept our model's synchrony control parameter, SharedProb, across values of 0.0, 0.3, 0.6, and 0.9. As shown in **Figure 2**, we observed a direct linear relationship between the input parameter and the measured biological Synchrony Strength.

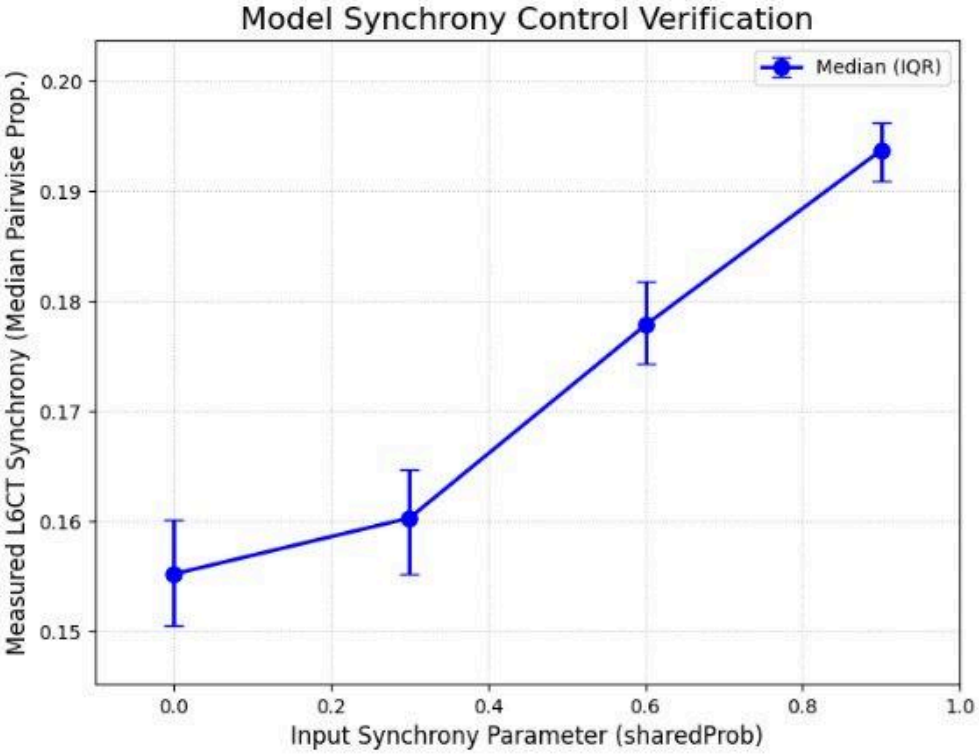

Figure 2: *Validation of the model's synchrony control. The input parameter (sharedProb) correlates linearly with the measured pairwise synchrony strength, confirming that we can manipulate temporal alignment without altering firing rate. The error bars represent the Interquartile Range (IQR), spanning the 25th to 75th percentiles of the measured synchrony distribution across all neuron pairs, while the central markers indicate the median synchrony strength.*

3.2 Replication of the "Window of Opportunity"

3.2 Replication of the "Window of Opportunity"

To replicate the biological mechanism, we simulated the full circuit dynamics while strictly controlling the L6CT input synchrony. To ensure the model captured the "race condition" between excitation and inhibition, we tuned the synaptic strength of the TRN-to-VPm pathway (P_max and PS_weight) and implemented gated conductance, which prevents the integration of synaptic currents while a neuron is in its refractory period.

Low Synchrony (P_sync = 0.0): When L6CT inputs were asynchronous, the TRN integrated the inputs effectively, creating a sustained "wall" of inhibition. As shown in the TRN PSTH, TRN firing rates rise rapidly to saturation (~200 Hz) even at low input synchrony. Consequently, the VPm received dispersed excitatory "kicks" that were insufficient to overcome this dominant inhibition, resulting in suppressed firing relative to baseline.

High Synchrony (P_sync = 0.9): When L6CT inputs were highly synchronous, they created large, transient excitatory conductances. Crucially, these excitatory peaks occurred before the delayed inhibitory conductance from the TRN could rise. This temporal gap—the "Window of Opportunity"—allowed the VPm to spike reliably for a short timescale before being silenced by the TRN.

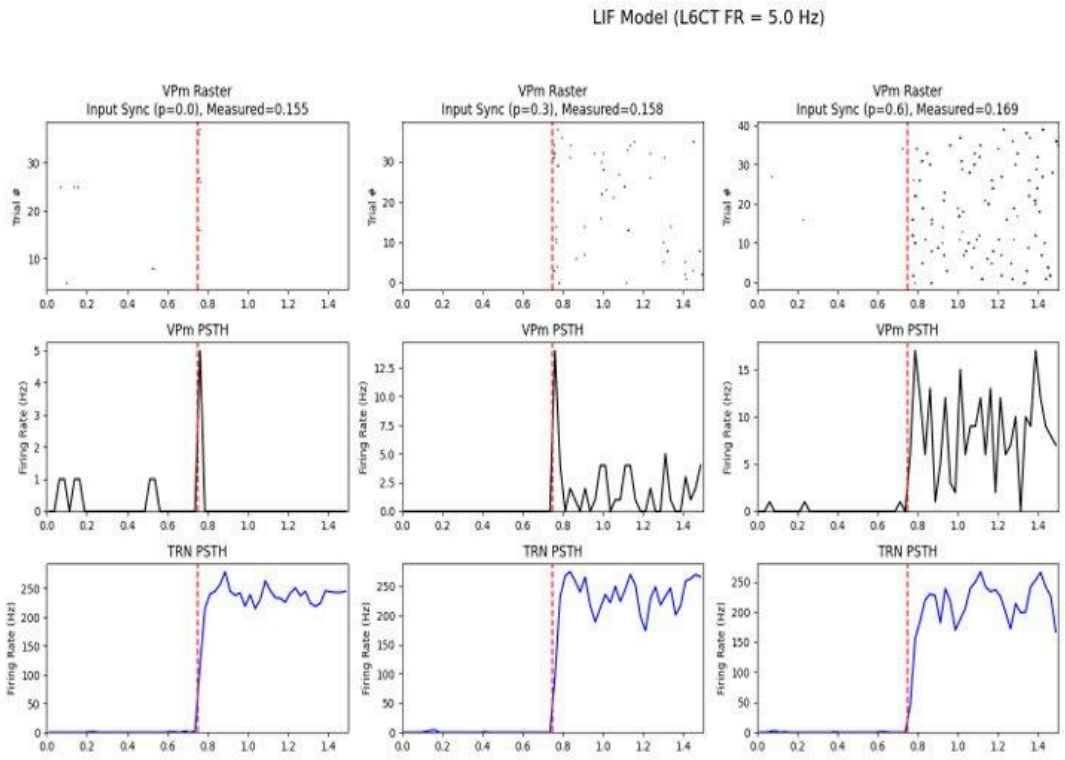

Figure 3: Summary of Population Dynamics across Synchrony Levels *VPm Rasters show a transition from sparse, random spiking at low synchrony (P=0.0) to dense, reliable spiking at high synchrony (P=0.9). Note that "Measured" values indicate the biological synchrony strength validated in Figure 2. (Middle Row): VPm PSTH confirms that firing rate increases significantly with synchrony*

(enhancement), despite the input firing rate remaining constant. (Bottom Row): TRN PSTH reveals that TRN firing saturates (~200 Hz) quickly. Most Importantly, TRN rate does not change drastically between P=0.6 and P=0.9, yet VPm firing does. This confirms that VPm enhancement is driven by input timing (VPm excitation beating the TRN inhibition), not by a lack of inhibition strength.

The Spike-Triggered Conductance (STC) analysis (Figure 3, bottom row) confirms the mechanism: as synchrony increases, the excitatory slope becomes steeper, outpacing the inhibition delay.

To visualize this fine-scale timing, we computed the Spike-Triggered Conductance (STC), which averages the excitatory and inhibitory conductances aligned to the moment a VPm neuron spikes as shown in Figure 4. At low synchrony, the excitatory drive is weak and slow, barely surpassing inhibition. However, at high synchrony, the STC reveals a sharp excitatory peak (green) that precedes the inhibitory peak (blue) by several milliseconds. This confirms that spiking is driven by the steep slope of synchronous excitation outpacing the synaptic delay of the TRN loop.

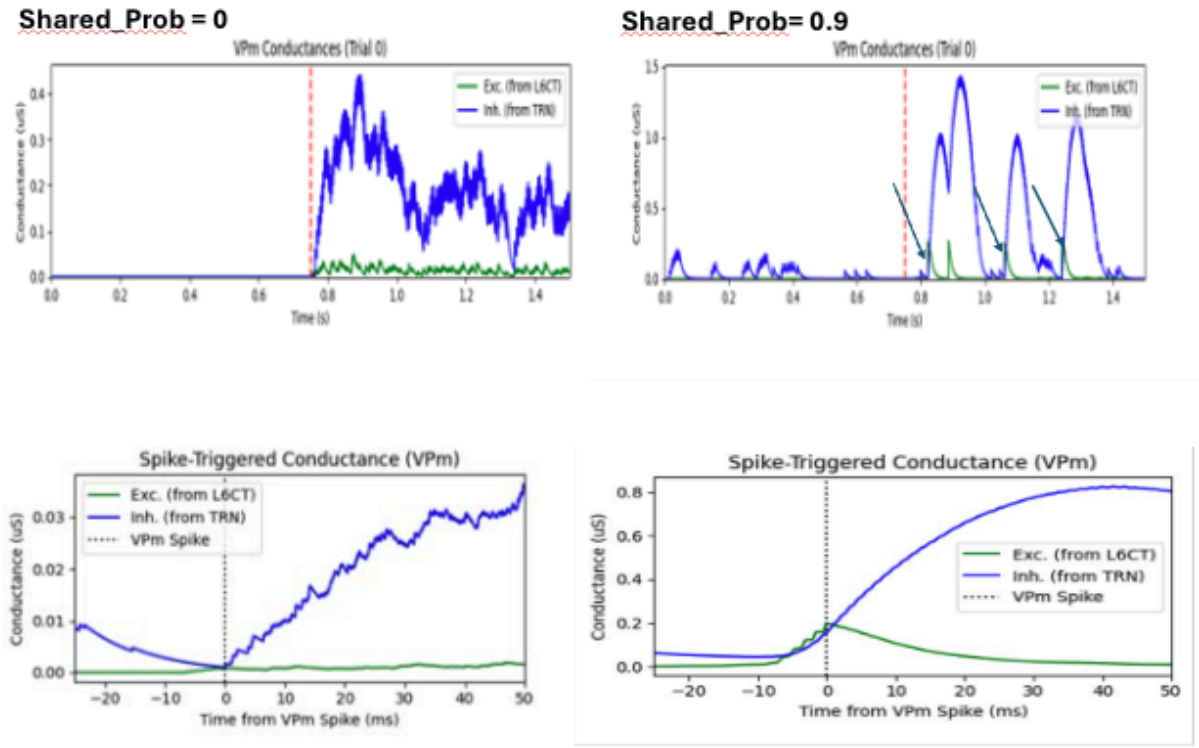

Figure 4: *Single-Trial Dynamics and Spike-Triggered Conductance. (Top Row): Single-trial traces of VPm conductance over the full stimulation window. At P=0.9, large gaps (indicated by arrows) appear where excitation (green) transiently exceeds inhibition (blue). (Bottom Row): Spike-Triggered Conductance (STC). These plots zoom in on the micro-timescale (±50 ms) centered on a VPm spike (t=0). They reveal the average shape of inputs required to drive a spike: at high synchrony, a sharp excitatory input precedes the inhibitory response, creating a magnified view of the temporal window for VPm firing.*

4. Extension: Linking VPm Synchrony to Cortical LFP Oscillations

4.1 Background and Objectives

As mentioned in the Introduction, the study by Russo et al. [2] aimed to investigate the relationship between Layer 6 corticothalamic (L6CT) neurons and the emergence of high-gamma oscillations in the cortical local field potential (LFP). The authors found that activation of S1 L6CT neurons induced high-frequency LFP oscillations in S1 whose frequency, but not amplitude, varied across light intensities and over time. By directly probing the roles of VPm and S1 cortical layers, they concluded that LFP oscillation frequency selectively correlates with the firing rate of VPm neurons.

Importantly, the biological results suggested that intracortical connections initially suppress cortical spiking, but that activity within the cortico-thalamic loop evolves rapidly, eventually leading to a facilitation of cortical spiking at later time points. Their findings showed that increases in L6CT firing were accompanied by corresponding increases in LFP oscillation frequency. Moreover, examining the dynamics of intracortico-thalamic neurons revealed that VPm neurons tended to facilitate at higher stimulus frequencies while being suppressed at lower intensities.

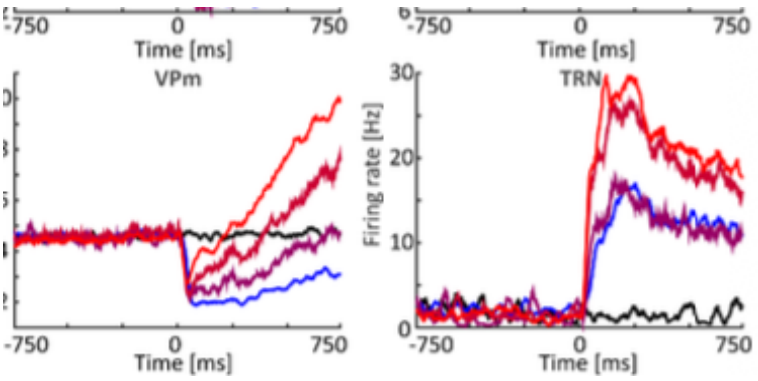

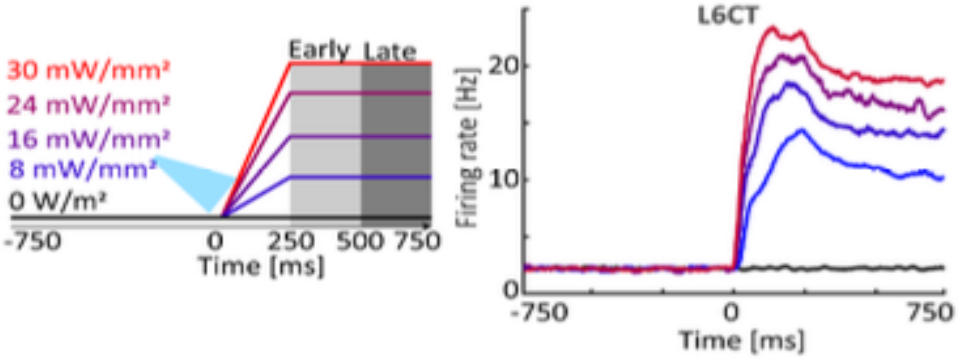

Figure 5: Experimental Benchmark. The effects of varying ramp-and-hold light intensities on L6CT firing rates and VPm/TRN spiking, as reported in [2]. Our model aims to capture the transition from suppression to facilitation observed in the VPm traces (bottom left).

4.3 LFP Results

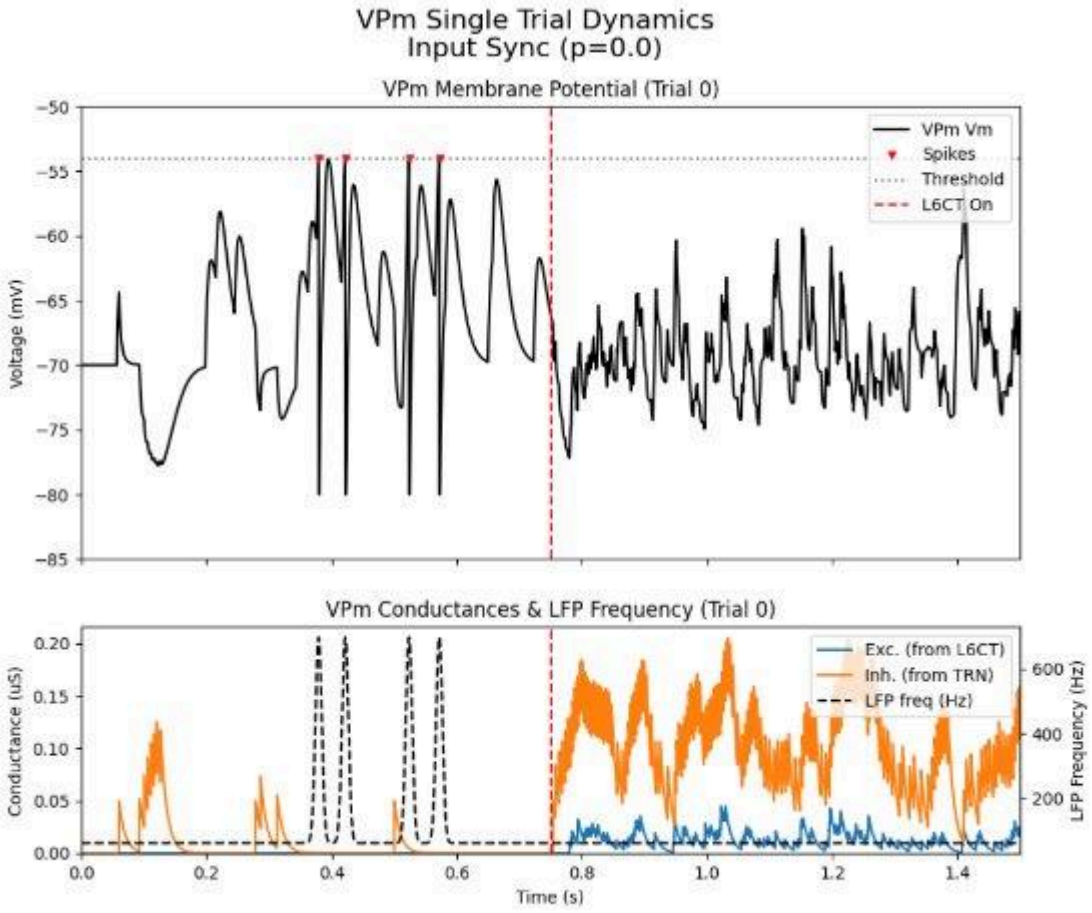

4.2 Computational Implementation

Our primary objective in this extension was to model VPm behavior as a function of different synchrony levels, based on the premise that higher L6CT synchrony produces a more favorable window for VPm excitation.

To simplify our model for this specific task, we collapsed all cortical layers into a single effective layer and focused primarily on the relationship between firing-rate modulation and thalamic neuron dynamics. As a result, our model represents a simplified account of how VPm neurons influence LFP modulation, capturing the transition from short-term suppression to long-term excitation observed in the experimental data.

Given the established role of L6CT synchrony in shaping thalamic excitability, we sought to examine how varying levels of L6CT synchrony influence LFP modulation. To address this, we adapted the integrate-and-fire neuron model described in the previous section to generate VPm spike trains with controlled synchrony, while imposing additional constraints to ensure consistency with the experimental observations.

The following code snippet illustrates the implementation of this functionality, where the instantaneous VPm firing rate is mapped to a time-varying frequency component of the LFP signal.

```python
def run_lif_simulation(config, l6ct_spike_trains_all_trials):

    # --------- Build VPm-driven synthetic high-gamma LFP per trial using that trial's PSTH --------- #
    times = np.arange(num_steps) * tStep

    for trial in range(nTrials):
        vpm_spikes_trial = all_output_spikes[trial, 1, :]  # boolean
        # Shape (1, num_steps) so we can reuse make_psth
        spikes_for_psth = vpm_spikes_trial[np.newaxis, :]

        psth_time, psth_rate = make_psth(spikes_for_psth, config)

        if len(psth_time) == 0:
            # No spikes at all: flat baseline frequency & zero signal
            freq_baseline = vpm_to_lfp_freq(5.0)  # rate=5 Hz → baseline f0
            lfp_freq_trial = np.ones(num_steps) * freq_baseline
            lfp_signal_trial = np.zeros(num_steps)
        else:
            # Map PSTH-derived rate to frequency at bin centers
            lfp_freq_bins = vpm_to_lfp_freq(psth_rate)
            # Interpolate onto full time axis
            lfp_freq_trial = np.interp(times, psth_time, lfp_freq_bins,
                                       left=lfp_freq_bins[0],
                                       right=lfp_freq_bins[-1])

            # Generate LFP oscillation with time-varying frequency
            lfp_signal_trial = np.zeros(num_steps)
            phase = 0.0
            for t in range(num_steps):
                freq = lfp_freq_trial[t]
                phase += 2 * np.pi * freq * tStep
                lfp_signal_trial[t] = np.sin(phase)

        all_lfp_signal[trial, :] = lfp_signal_trial
        all_lfp_frequency[trial, :] = lfp_freq_trial
```

Snippet 2: Python implementation of the LFP generation pipeline. The code extracts the PSTH from the VPm output and maps the firing rate to a sinusoidal frequency to generate synthetic LFP oscillations.

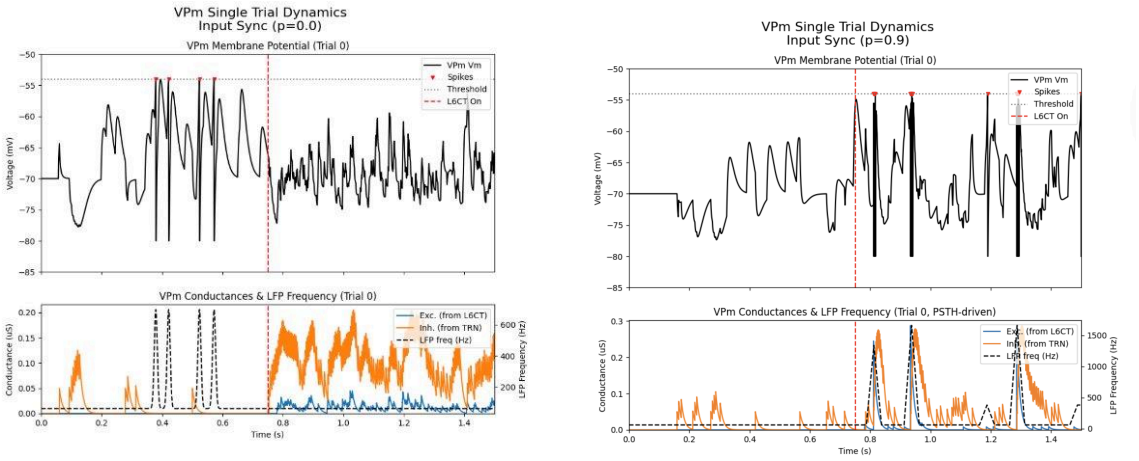

Figure 7: Simulation of Cortical LFP. (Left) Low Synchrony (P=0.0): *The VPm firing rate remains suppressed or near baseline due to dominant TRN inhibition. Consequently, the modeled LFP frequency remains constant and low.* ***(Right) High Synchrony (P=0.9$:*** *The "window of opportunity" allows the VPm to escape inhibition and fire robustly (high peaks in the PSTH). This sharp increase in VPm firing rate drives a rapid up-chirp in the generated LFP signal (bottom trace), reproducing the high-gamma frequency shifts observed in the biological dataset.*

Our simulation results support the hypothesis that L6CT synchrony is a control parameter for cortical oscillation dynamics.

- **Low Synchrony:** The VPm firing rate remains suppressed or near baseline. Consequently, the modeled LFP frequency remains constant and low.
- **High Synchrony:** The "window of opportunity" allows the VPm to escape inhibition and fire robustly. This sharp increase in VPm firing rate drives a rapid up-chirp in the generated LFP signal, reproducing the high-gamma frequency shifts observed in the Russo et al. dataset.

5. Discussion

Our computational model successfully replicates the counter-intuitive finding that thalamic throughput is not merely a function of input magnitude, but of input *timing*. By mathematically isolating synchrony from firing rate, we confirmed that the L6CT-TRN-VPm circuit acts as a temporal filter. Asynchronous inputs recruit dominant inhibition (suppression), while synchronous inputs exploit the synaptic delay to drive spiking (enhancement) .

The extension of our model to LFP oscillations bridges the gap between cellular dynamics and network states. It suggests a causal chain: **L6CT Synchrony → VPm Window of Opportunity → VPm Firing Rate → Cortical LFP Frequency.** This implies that the cortex can dynamically tune the frequency of its own oscillatory state by modulating the temporal alignment of its feedback projections to the thalamus.

References

[1] Dimwamwa, E. D., Pala, A., Chundru, V., Wright, N. C., & Stanley, G. B. (2024). Dynamic corticothalamic modulation of the somatosensory thalamocortical circuit during wakefulness. *Nature Communications*, *15*, 3529.

[2] Russo, S., Dimwamwa, E. D., & Stanley, G. B. (2025). Layer 6 corticothalamic neurons induce high gamma oscillations through cortico-cortical and cortico-thalamo-cortical pathways. *bioRxiv*.